Available online at www.sciencedirect.com
SCIENCE DIRECT®
Agricultural and Forest Meteorology 127 (2004) 189–201
AGRICULTURAL AND FOREST METEOROLOGY
www.elsevier.com/locate/agrformet

Evaluation of Lagrangian footprint model using data from wind tunnel convective boundary layer

N. Kljun[a,*], P. Kastner-Klein[b], E. Fedorovich[b], M.W. Rotach[a,1]

[a]*Institute for Atmospheric and Climate Science (IAC), ETH, Winterthurerstr. 190, CH-8057 Zurich, Switzerland*
[b]*School of Meteorology, University of Oklahoma, Norman, OK, USA.*

Accepted 15 July 2004

Abstract

The Lagrangian footprint model LPDM-B was evaluated using data from SF_6 tracer release experiments in a wind tunnel with a sheared convective boundary layer. The evaluation considered both the dispersion module and the footprint predictions of LPDM-B. It was found that the dispersion patterns and the concentration footprints compared well with the wind-tunnel data. The footprint model was able to reproduce the observed peak location and the shape of the footprint estimates for various sampling heights throughout the entire boundary layer. Furthermore, a comparison of two footprint model approaches ('forward-in-time' and 'backward-in-time' trajectories) was carried out using the same core model. This comparison revealed that the two approaches may not necessarily result in the same footprint estimate and also were very sensitive to the height-dependent performance of the applied dispersion module.

Keywords: Atmospheric boundary layer; Convection; Footprint; Lagrangian simulation; Turbulence statistics; Wind tunnel

1. Introduction

In recent years, several footprint models for flux or concentration measurements have been proposed (see Schmid, 2002, for a review). However, validation of footprint models still is an open question. In several studies, analytical footprint predictions have been compared with footprint estimates of the Lagrangian type, whereby the latter have been usually taken as a reference (e.g., Leclerc and Thurtell, 1990; Schuepp et al., 1990; Wilson and Swaters, 1991; Horst and Weil, 1992, 1994; Baldocchi, 1997; Rannik et al., 2000). Yet, whether the footprint estimates from different approaches agree or not, suitable experimental data are necessary to decide whether the footprint models yield the correct predictions. So far, only few studies compared data of tracer release experiments or airborne data with footprint model results (Finn et al., 1996; Leclerc et al., 1997; Kaharabata et al., 1997; Leclerc et al., 2003a,b).

* Corresponding author. Fax: +41 1 362 5197.
E-mail address: nkljun@ethz.ch (N. Kljun).
[1] Present address: Swiss Federal Office of Meteorology and Climatology, MeteoSwiss, Zurich, Switzerland.

0168-1923/$ – see front matter © 2004 Elsevier B.V. All rights reserved.
doi:10.1016/j.agrformet.2004.07.013

However, there is still a lack of reliable full-scale data. The reason often lies in the constraints that the model assumptions require (e.g., restriction to the surface layer). In particular, stationary turbulence and horizontal homogeneity are fundamental requirements for evaluation studies of footprint approaches and are difficult to meet in the field. Some footprint models were tested against data of complex flows, as, for example, dispersion inside and above forest canopies (e.g., Kaharabata et al., 1997; Leclerc et al., 2003a,b). However, such plant canopy data may not be ideal for a first evaluation of general footprint models, because the canopy itself influences the velocity statistics. These in turn control the vertical dispersion and thus the characteristics of the footprint estimate. Here we advocate first validating our footprint model under ideal, controlled conditions before moving on to more complicated situations.

The requirements of stationary turbulence and, if necessary, homogeneous surfaces can easily be fulfilled in wind-tunnel or water-tank experiments. In addition, measurements in laboratory studies can be performed with high spatial and temporal resolution. Wind-tunnel data have been successfully employed for evaluation purposes of dispersion models (e.g., Kurbanmuradov and Sabelfeld, 2000). Thus it can be expected that they are similarly well suited for an evaluation of footprint models. Only recently, results from convective dispersion experiments have been presented using wind-tunnel experiments performed at the University of Karlsruhe, Germany, to provide vertical and lateral dispersion data (Fedorovich and Thäter, 2002). The flow and turbulence characteristics in this wind tunnel have been intensively investigated and compared well with atmospheric data (Fedorovich et al., 1996). Since convective boundary layers (CBL) represent the majority of conditions met during daytime in the field, this wind tunnel provides an ideal set-up for evaluation of footprint models. Accordingly, the present study focuses on the evaluation of the 3D Lagrangian footprint model LPDM-B of Kljun et al. (2002), using these wind-tunnel data.

The evaluation of LPDM-B was performed in three steps: first, the dispersion module that LPDM-B was based upon was validated against the wind tunnel data; second, the same was done for the footprint predictions of LPDM-B; third, the two footprint approaches of Lagrangian particle models were compared, namely those based on (i) 'forward-in-time' trajectories and (ii) 'backward-in-time' trajectories.

2. Model description

2.1. Footprint model

In the present study, footprint estimates were derived using the three-dimensional Lagrangian stochastic footprint model LPDM-B of Kljun et al. (2002). As in all Lagrangian particle models, the emitted tracer was simulated as the release of a large number of particles, which were assumed to follow the flow exactly. The diffusion of the scalar was described by a stochastic differential equation (a generalised Langevin equation) which determines the motion of a Lagrangian particle in space and time (Thomson, 1987). Unlike most other Lagrangian stochastic particle models, the present model is not only valid in one given stability regime, but was designed for boundary layer conditions from stable to convective, and therefore it is valid for application within a broad range of boundary layer flow types. LPDM-B is thus able to account for both shear and buoyant turbulence production.

In LPDM-B, particles are tracked backwards in time, from the measurement location to the source (e.g., at the surface), using 'backward' trajectories of particles as described in Flesch et al. (1995). The footprint for a measured concentration or flux at a given sampling height and location was determined as proposed in Flesch et al. (1995) and Flesch (1996). This approach permits calculation of the footprint for a *measurement point* instead of an average over a sensor volume. Furthermore, it is not dependent on a coordinate transformation that would require horizontal homogeneity of the flow. So far, LPDM-B has been tested against results of other footprint models in terms of flux and concentration footprints (Kljun et al., 2002, 2003). In the present study, only concentration footprints were considered, since no flux measurements were available from the wind-tunnel experiment. For a complete description of LPDM-B, the reader is referred to Kljun et al. (2002).

2.2. Dispersion module

In the following sections, special emphasis is given to the dispersion module of LPDM-B: the turbulence and diffusion characteristics employed in LPDM-B are similar to those of the three-dimensional Lagrangian stochastic particle dispersion model developed by Rotach et al. (1996) and de Haan and Rotach (1998). This dispersion module (below denoted as DMOD) has been tested extensively and compared to water-tank and field data. Rotach et al. (1996) compared the results of the dispersion module to the water-tank experiments of Willis and Deardorff (1976, 1978, 1981) and showed that in free convection conditions, the model is able to qualitatively and quantitatively reproduce the features of the dispersion process for sources at different heights. For stability conditions between neutral and strongly convective, the dispersion module has been shown (Rotach et al., 1996) to successfully reproduce both field data from a full-scale tracer experiment in Copenhagen and results from large eddy simulations by Mason (1992). Most recently (Rotach, 2001), the model has been tested against the stable runs of the 'Prairie Grass' experiment as reported in Van Ulden (1978), and again, no pronounced bias or scatter has been detected.

The present wind-tunnel dataset provides yet another opportunity to evaluate the dispersion module of LPDM-B. Furthermore, if the dispersion processes observed in the wind tunnel are well reproduced by the dispersion module of LPDM-B, any observed discrepancies between the wind-tunnel data and the footprint estimates of LPDM-B will be mainly due to the footprint derivation employed in LPDM-B. Simulations of DMOD allow for calculations of footprint estimates using 'forward-in-time' trajectories (see Section 4). Thus, the two different approaches used in Lagrangian footprint modelling can also be compared.

2.3. Turbulence parameterisations

As a Lagrangian particle model, LPDM-B permits the easy modification of the turbulence parameterisations to correspond to the observed conditions. The present wind-tunnel experiments (Section 3) provide high-resolution data of the mean flow parameters and turbulence statistics. In order to reproduce the wind-tunnel flow as accurately as possible, the turbulence parameterisations of LPDM-B (see Rotach et al., 1996) were, for the present study, adapted to the corresponding turbulence statistics measured in the wind tunnel (Fedorovich et al., 1996; Kaiser and Fedorovich, 1998).

For each parameterisation, two wind-tunnel profiles were considered, measured 2.3 and 4.0 m downwind of the tracer source location (Fedorovich and Thäter, 2002). A comparison with the model profiles showed that the wind-tunnel profiles of mean wind speed, $\bar{u}$, and of Reynolds stress, $\overline{u'w'}$, were well represented by the original parameterisations. Substantial differences were found for the parameterisations of longitudinal, lateral, and vertical velocity variances, the vertical velocity skewness, and the dissipation rate of turbulence kinetic energy. Accordingly, the parameterisations for these turbulence statistics were fitted to the wind-tunnel observations (Fig. 1) and implemented in LPDM-B. Note that these new parameterisations were not based on any physical principles, but were merely a fit to the observations.

As will be mentioned in Section 3, the CBL generated in the wind tunnel was capped by a temperature inversion. This inversion was relatively weak and therefore not completely impermeable for the tracer. Several simulations with different reflection schemes led to the assumption that this behaviour was being taken into account by using the turbulence profiles as derived from the wind-tunnel observations. No reflection was therefore imposed on the particles as they reached the boundary layer top.

3. Wind-tunnel experiments

The wind tunnel at the University of Karlsruhe, Germany, was specially designed for simulations of gaseous pollutants dispersion in the CBL capped by a temperature inversion (Fedorovich et al., 1996; Fedorovich and Thäter, 2002). In contrast to traditional laboratory water-tank simulations, where only a shear-free CBL is considered, these experiments provide data for the combined effects of buoyancy and shear forcing in a CBL flow with a shear/buoyancy production ratio of $u_*/w_* \approx 0.2$ (u_* denoting the friction velocity and w_* the convective velocity scale). The flow characteristics in the tunnel have been widely

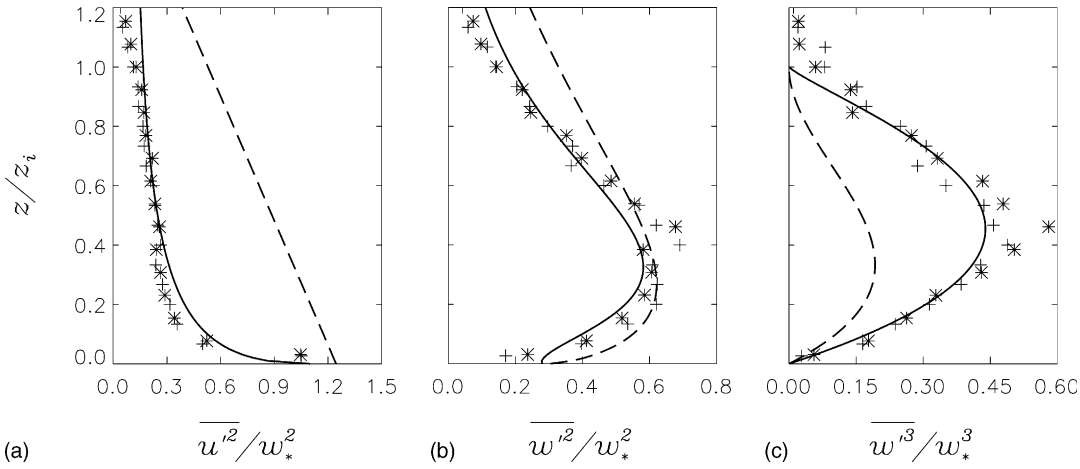

Fig. 1. Turbulence profiles for (a) longitudinal velocity variances, (b) vertical velocity variances, and (c) vertical velocity skewness of LPDM-B as derived from the wind-tunnel data (solid line), LPDM-B's original profiles (dashed line), and wind-tunnel observations at 2.3 m (*) and at 4.0 m (+) downwind of the source vs. height z/z_i.

compared with field data, other laboratory data and numerical simulations. These studies have shown that the wind tunnel is a reliable tool to simulate atmospheric, convective boundary layers.

The thermally stratified wind tunnel was of the closed-circuit type. The return section of the tunnel was subdivided into 10 layers, each of them driven by its own fan. The two lowest layers were operated in an open-circuit regime. Thus it was possible to enforce quasi-stationary inlet conditions for the flow entering the test section while insuring proper CBL development and tracer dispersion. The test section of the tunnel had the dimensions 10 m × 1.5 m × 1.5 m, with a relatively smooth underlying surface (Table 1). The floor of the test section was heated to produce a constant kinematic heat flux through the bottom of the CBL of approximately 1 K m s^{-1}. This procedure resulted in strong convection with shear remaining very important (Table 1). For a detailed description of the wind-tunnel experiment see Fedorovich et al. (1996) and Fedorovich and Thäter (2002).

For the tracer experiment, SF_6 was isokinetically released from a pipe outlet mounted horizontally inside the simulated CBL at ground-level $z/z_i \approx 0.0$ (z denoting the height above ground and z_i the boundary layer height). The diameter of the pipe outlet was 1 mm. The point source was placed in the central vertical plane of the tunnel, 3.32 m downwind of the tunnel inlet. The release rate of the tracer was adjusted to the optimal range of the detector of 5–100 ppm, i.e., for measurements close to the source less SF_6 was released than for measurements further downwind. For the present study, the measured concentrations were normalised by the source rate.

Concentration measurements were carried out every 0.03 m between the heights of z = 0.00 and 0.33 m, and at varying distances from the source, x (m) = [0.33, 0.66, 0.99, 1.32, 1.65, 1.98, 2.31, 2.86, 3.40, 3.96]. At the lowest level, z = 0.00 m, concentrations were also measured in the crosswind direction every 0.04 m between y = 0.00 and 0.68 m. The measurements were averaged over periods of 2-min duration.

Table 1
Mean wind speed, $\bar{u}$, velocity scales, u_* and w_*, boundary layer height, z_i, Obukhov length, L, roughness length, z_0, sensible heat flux, H, and convective Richardson number, $Ri_{\Delta T}$, characterising the wind-tunnel flow and the corresponding 'atmospheric' flow in LPDM-B

	$\bar{u}$ (m s^{-1})	u_* (m s^{-1})	w_* (m s^{-1})	z_i (m)	L (m)	z_0 (mm)	H (W m^{-2})	$Ri_{\Delta T}$ (–)
Wind tunnel	1.0	0.076	0.18	0.35	−0.067	0.1	615	5
Atmosphere	11.6	0.88	2.08	700.0	−133.6	200	480	5

For each measurement profile, 20 air samples were simultaneously collected in small, airtight cylinders. Each sample was then individually passed to the detector and analysed. The total time for collection and analysis of 20 samples was about 30 min. Tracer concentrations were measured with an electron capture detector (LH108, Meltron Qualitek Messtechnik GmbH, Germany). This detector ionises a carrier gas (Argon) which then produces a permanent current. The electronegative SF_6 captures electrons while passing the detector and thus reduces the current. The detector was calibrated regularly against gas samples of known concentration. The flow velocity components were measured with a laser Doppler system. Background concentration was monitored upwind of the source and no significant accumulation of SF_6 was observed during the experiment.

The errors in measuring the concentrations were in the order of 10%. Additionally, uncertainties occurred due to imprecise positioning of the sampling probes. These uncertainties, however, were difficult to quantify since a small shift of the sampling point (order of mm) in regions of large vertical and horizontal gradients caused a much higher error than the same shift in a well-mixed region.

4. Methods and simulations

Most of the Lagrangian footprint models are principally 'forward-in-time' dispersion models (e.g., Leclerc and Thurtell, 1990; Horst and Weil, 1992; Rannik et al., 2000). When applying this footprint approach, the particles are released at a ground-level point source and advected downwind, as done in dispersion models. For a given stability condition and measurement height, the footprint value depends only on the separation d between the observation position and the source. The modelled concentration patterns can thus be transformed into footprint predictions by sampling at the measurement height. In other words, the 'forward' footprint was estimated by adding up the particle contributions according to their positions when the particle trajectories pass the measurement height (in either direction).

The main difference between the 'forward' approach and the 'backward' approach as applied by LPDM-B is that in the latter, the particles are released at the measurement position and the particles are tracked backwards in time (after suitable changes in the equations for the velocity increments, see Kljun et al., 2002). Different from the 'backward' approach, where the calculated trajectories can be used directly, the 'forward' footprint is usually computed after a coordinate transformation and therefore requires horizontal homogeneity of the flow.

The wind-tunnel dispersion experiment provides concentration measurements at several heights and positions downwind of the ground-level point source. The boundary layer of the wind-tunnel refers to the case of a quasi-stationary, horizontally evolving CBL (Fedorovich et al., 1996). However, at the source location, the CBL flow has already evolved and can be considered as approximately horizontally homogeneous in the main part of the test sections. The surface of the wind tunnel was clearly homogeneous, sidewall effects due to reflection of the tracer were negligible. Horst and Weil (1992, 1994) showed that the footprint was equal to the spatial distribution of the flux or concentration downwind of a unit ground-level point source. When applying a coordinate transformation similar to the one used for the 'forward' footprint approach and assuming horizontally homogeneous flow, the set-up of the wind tunnel was hence equivalent to a dispersion experiment of a single measurement position downwind of a surface source (cf. Leclerc et al., 2003b).

LPDM-B was designed to simulate real-scale flow. Thus, in order to compare wind-tunnel data with results of LPDM-B, the flow parameters characterising the atmospheric counterpart of the wind-tunnel flow were determined (Table 1). As similarity criteria, the ratio between friction velocity and convective velocity u_*/w_* and the convective Richardson number, $Ri_{\Delta T}$, were used. The convective Richardson number was based on the temperature difference ΔT across the inversion layer and given as

$$Ri_{\Delta T} = \beta w_*^{-2} z_i \Delta T$$

where $\beta = g/T_0$ is the buoyancy parameter, g denotes the acceleration due to gravity and T_0 the reference temperature. The temperature difference across the inversion was 30 K in the wind tunnel and set to 2 K for the atmospheric flow. The scaling factor for the length scales was based on the observed boundary

layer height, z_i, of the wind tunnel and a reasonable value for z_i in the atmosphere. For the present study, the length-scale ratio was set to $z_{i,\mathrm{atmos}}/z_{i,\mathrm{wt}} = 2000$.

The resulting atmospheric flow parameters (Table 1) were used as input parameters for LPDM-B and its dispersion module (DMOD).

Fedorovich et al. (1996) showed that the scaled mean flow parameters and the turbulence statistics of their wind-tunnel experiments compared well with their atmospheric counterparts. Thus, to assess the adequacy of the actual turbulence parameterisations and to test the sensitivity of the simulations on the latter, model runs were performed with the original turbulence parameterisations as of Rotach et al. (1996) and with modified parameterisations as described in Section 2.3. Predicted surface concentrations, mean plume characteristics, and ensemble-averaged concentration profiles were calculated from the results of DMOD. Footprint estimates ('forward' and 'backward' approach) were calculated for the measurement heights $z_m/z_i = [0.09, 0.17, 0.26, 0.34, 0.43, 0.51, 0.60, 0.69, 0.77, 0.86, 0.95]$ corresponding to the heights of concentration measurements in the wind tunnel (no footprint calculation for the ground-level measurement).

The results of all simulations are presented in normalised form using the Deardorff scales (Deardorff, 1985). The dimensionless concentration C_* along the plume centreline ($y = 0$) and the dimensionless crosswind-integrated concentration, CIC_*, were given by

$$C_* = \frac{C\bar{u}z_i^2}{Q}$$

$$\mathrm{CIC}_* = \frac{\mathrm{CIC}\bar{u}z_i}{Q}$$

where C denotes the actual centreline concentration, $\bar{u}$ the mean wind speed in the wind tunnel, and Q the source emission rate. CIC denotes the actual crosswind-integrated concentration with

$$\mathrm{CIC} = \int_{-\infty}^{\infty} C(x, y, z)\,\mathrm{d}y$$

The distance downwind of the source was normalised according to

$$X_* = \frac{xw_*}{z_i\bar{u}}$$

where x denotes the actual distance from the point source at $x = 0$. The integral of a flux footprint is defined to approach unity. This is not the case for concentration footprints. Thus, in order to compare wind-tunnel results with the concentration footprints predicted by LPDM-B, the latter were normalised using the integral concentration of the wind-tunnel footprint such that

$$\int_D f_{C_{\mathrm{mod}}}\,\mathrm{d}X_* = \int_D f_{C_{\mathrm{obs}}}\,\mathrm{d}X_*$$

where f_C denotes the concentration footprint function, C_{obs} the observed concentration, C_{mod} the corresponding predicted value, and D the plume centreline between first and last measurement position.

Summary statistics as proposed by Hanna et al. (1993) were calculated to evaluate the performance of the footprint model:

R	correlation between C_{mod} and C_{obs}
F_2	percentage of C_{mod} within a factor of 2 of C_{obs}, $F_2 = 100\,n_2/n$
F_B	Fractional bias, given as $F_B = 2(\bar{C}_{\mathrm{obs}} - \bar{C}_{\mathrm{mod}})/(\bar{C}_{\mathrm{obs}} + \bar{C}_{\mathrm{mod}})$
$\varepsilon_{\mathrm{NMS}}$	normalised mean square error, $\varepsilon_{\mathrm{NMS}} = \overline{(C_{\mathrm{obs}} - C_{\mathrm{mod}})^2}/\overline{(C_{\mathrm{obs}}C_{\mathrm{mod}})}$

where n is the number of data points, and n_2 the number of data points for which $1/2C_{\mathrm{obs}} \leq C_{\mathrm{mod}} \leq 2C_{\mathrm{obs}}$. Overbars indicate average values of the respective dataset.

5. Results and discussion

5.1. Dispersion patterns

We start with the dataset that is typically available to dispersion modellers for validation purposes: surface observations such as crosswind-integrated ground-level concentrations (CIC) and the mean plume characteristics such as mean plume height and mean plume depth. Fig. 2 compares results of the DMOD simulations with the wind-tunnel data and exhibits good agreement between the two. Even though the mean plume height as simulated successfully approaches the equilibrium height, $\bar{z}/z_i = 0.5$, at

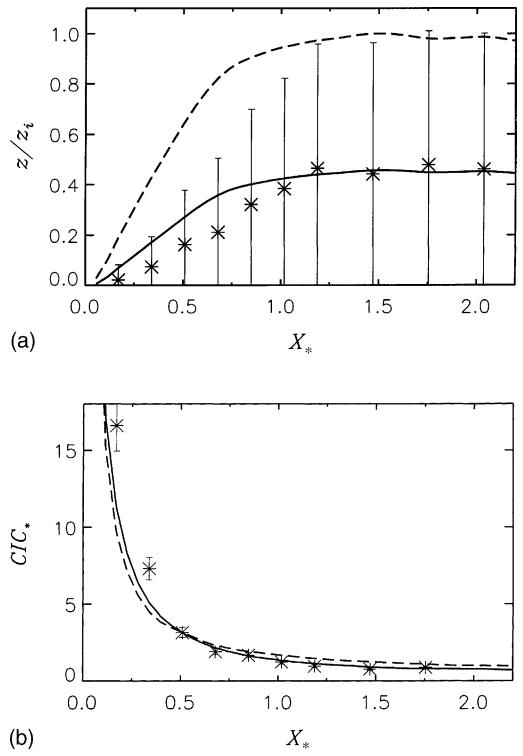

Fig. 2. (a) Mean plume height as measured (*) and predicted by DMOD downwind of a ground-level point source. The vertical depth of the plume (expressed as the variance of the particle distribution) is denoted as a dashed line (DMOD) and bars (observations), respectively. (b) Crosswind-integrated ground-level concentration CIC_* as measured (*, bars denote measurement errors) and as predicted by DMOD using the wind tunnel fitted turbulence parameterisations (solid line) and the original turbulence parameterisations (dashed line).

$X_* \approx 4$ (not shown), it was somewhat overestimated close to the source (Fig. 2a). This means that DMOD produces too strong dispersion close to the ground (see below). Fig. 2b confirms these findings: the model was capable of reproducing the CIC within the limits of experimental uncertainties except for regions close to the source, where the CIC was underestimated by the model.

In order to compare the dispersion patterns in more detail, vertical and horizontal concentration profiles measured in the wind tunnel and predicted by DMOD were analysed. Generally, the simulations coincide well with the observations (Fig. 3). However, the concentration profiles at $X_* = 0.17$ and at $X_* = 0.34$ again reveal that DMOD was not able to reproduce the observed high concentration peak at these small distances from the source. The initial near-surface dispersion close to the source was overestimated, while the observed surface concentrations further downwind, beyond $X_* = 0.34$, decreased much more rapidly than predicted by the model.

The strong concentration underestimation by DMOD close to the source might be due to a possible large bias in the observations when measuring in regions with large concentration gradients (cf. Section 3). Other possible reasons were the differences in source design in the wind-tunnel experiments and in the simulations. While the model referred to a fully turbulent plume in a turbulent flow, the plume in the wind tunnel might not be fully turbulent at source exit, but rather laminar. Such a plume would remain laminar for some short distance downstream of the source and lead to much higher concentrations than a turbulent plume.

At $X_* = 1.02$ and $X_* = 1.19$, DMOD predicted maximum concentrations close to the surface while the observed concentration maximum was found at higher elevations (z/z_i between 0.3 and 0.5). However, the magnitude of the concentrations was well predicted. For distances further downwind of the source ($X_* \geq 1.47$), the dispersion was well reproduced by DMOD. As expected, DMOD with turbulence parameterisations retrieved from the wind tunnel shows better correspondence to the observations than DMOD with the original turbulence parameterisations (Fig. 3). The latter predicted rather high concentrations close to the ground at $X_* \geq 0.51$.

The summary statistics calculated for the crosswind-integrated surface concentration and the concentration profiles confirm the good agreement of model and observations (Table 2). Rather large ε_{NMS} (>1) were produced by DMOD using fitted turbulence parameterisations. This was entirely due to the already discussed failure of the model to reproduce the very large concentrations observed near the source. If, for example, the lowest observation height at $X_* = 0.17$ and 0.34, respectively, was disregarded (see Fig. 3), the ε_{NMS} and F_B reduce to 0.35 and -0.09, respectively.

In summary, the present evaluation showed two aspects. First, if only the surface data were considered as usually done for model evaluation from full-scale data, the summary statistics and the corresponding

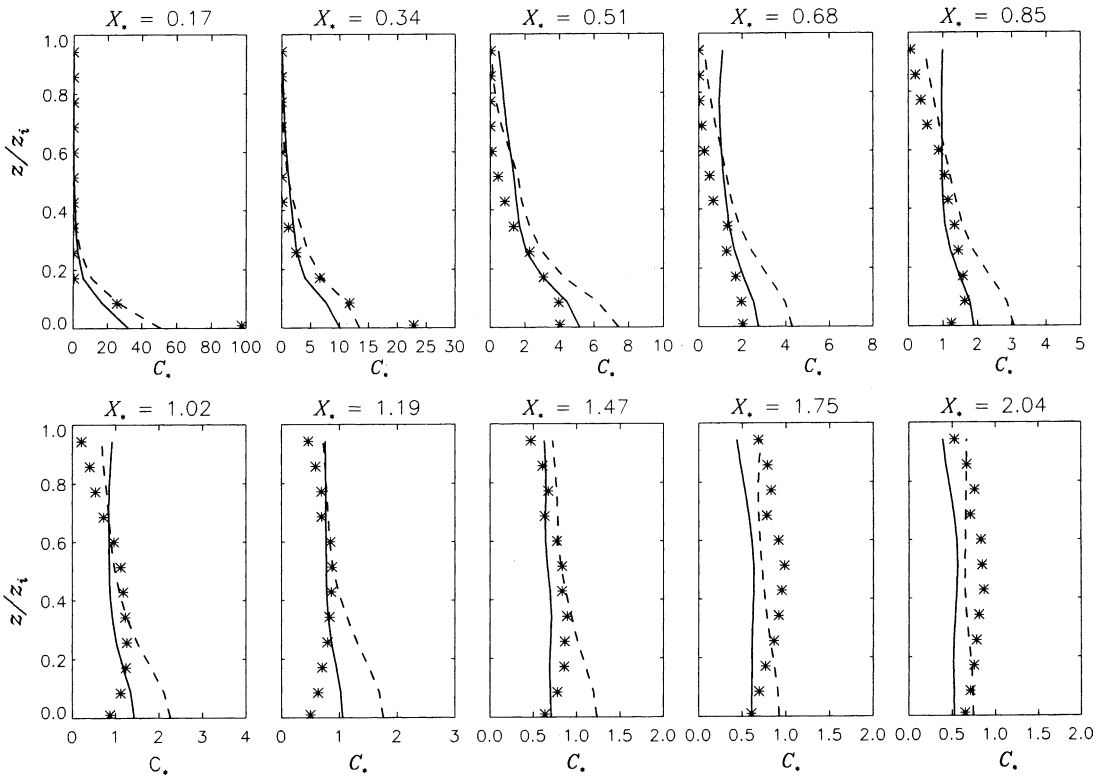

Fig. 3. Comparison of measured vertical concentration profiles (*) along the plume centreline ($y = 0$) downwind of the ground-level point source with profiles calculated by DMOD using the wind-tunnel fitted (solid line) and the original (dashed line) turbulence parameterisations. Note the varying concentration scales on the horizontal axes of the sub-figures.

Fig. 2 reveal excellent agreement between observation and numerical simulation. It seemed to be much more difficult for a dispersion model to actually match the entire concentration field as represented here through the various profiles in Fig. 3. However, using the observed (rather than the fitted) turbulence parameterisations, Fig. 3 shows that with the exception of the near-surface concentrations close to the source DMOD adequately reproduced the observations.

Table 2
Summary statistics for the crosswind-integrated *surface* concentration (10 data points) and vertical concentration *profiles* (104 data points) as predicted by DMOD using the wind-tunnel fitted (Fit) and the original (Orig) turbulence parameterisations

	CIC, surface		Profiles	
	Fit	Orig	Fit	Orig
R	1.0	0.99	0.95	0.95
F_2	100	100	79	73
F_B	0.11	0.12	0.16	0.00
ε_{NMS}	0.13	0.26	1.13	0.39

R denotes the correlation, F_2 the percentage of the predicted concentration within a factor of 2 of the observed concentration, F_B the fractional bias, and ε_{NMS} the normalised mean square error.

5.2. Footprint evaluation

In Fig. 4, the concentration footprints predicted by LPDM-B for the measurement heights $z_m/z_i \approx [0.1, 0.2, 0.5, 0.8]$ were compared with the respective observations. The measured concentration footprints compared well with results of LPDM-B in both peak location and footprint shape. For small measurement heights, LPDM-B was able to reproduce the peak location of the footprint, yet the peak value was underestimated (resulting in a rather high ε_{NMS}, see Table 3). Similar to the discrepancies between observation and DMOD results close to the source (Section 5.1), these differences might be due to

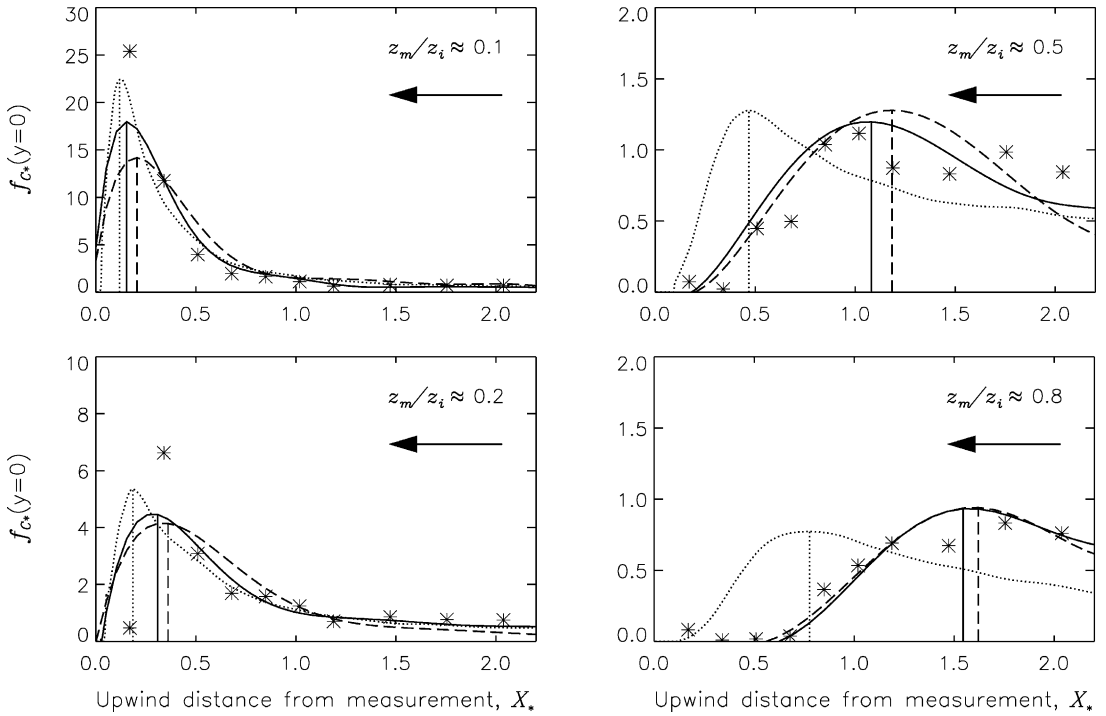

Fig. 4. Concentration footprint f_{C_*} at $y = 0$ as predicted by LPDM-B ('backward-in-time') using the turbulence parameterisations derived from the wind tunnel (solid line) and the original turbulence parameterisations (dashed line), by the 'forward-in-time' approach using the wind tunnel fitted turbulence parameterisations (dotted line), and as derived from the wind-tunnel experiment (symbols). Measurement heights are given for each sub-figure. The arrow indicates the wind direction and the vertical lines identify the peak location.

discrepancies in the source design, or due to the large uncertainty when measuring in regions with large concentration gradients.

The wind-tunnel data also allowed for the calculation of footprints for measurement heights above the surface layer (i.e., $z/z_i > 0.1$ and $-z/L > 1$). Such data are highly valuable for the evaluation, since distinct discrepancies in the footprint predictions of LPDM-B and analytical models were found when applying them for measurements above the surface layer, i.e., in conditions where analytical models should not be applied (Kljun et al., 2002, 2003). The results presented in Figs. 4 and 5a, and in Table 3 illustrate that LPDM-B agreed well with the observed footprint

Table 3
Summary statistics for the concentration footprints predicted by LPDM-B ('backward-in-time' approach) using the wind tunnel fitted (Fit) and original (Orig) turbulence parameterisations

	$z_m/z_i \approx 0.1$		$z_m/z_i \approx 0.2$		$z_m/z_i \approx 0.5$		$z_m/z_i \approx 0.8$		Total	
	Fit	Orig	Fit	Orig	Fit	Orig	Fit	Orig	Fit	Orig
R	0.98	0.92	0.71	0.70	0.84	0.81	0.93	0.97	0.96	0.91
F_2	100	91	91	73	82	73	64	64	78	75
F_B	0.05	0.04	−0.03	−0.02	−0.03	−0.02	0.01	0.00	0.00	0.02
ε_{NMS}	0.10	0.26	0.31	0.33	0.07	0.10	0.06	0.03	0.11	0.27

The number of data points for each measurement height is 11, and 121 when combining all 11 measurement heights. R denotes the correlation, F_2 the percentage of the predicted concentration within a factor of 2 of the observed concentration, F_B the fractional bias, and ε_{NMS} the normalised mean square error.

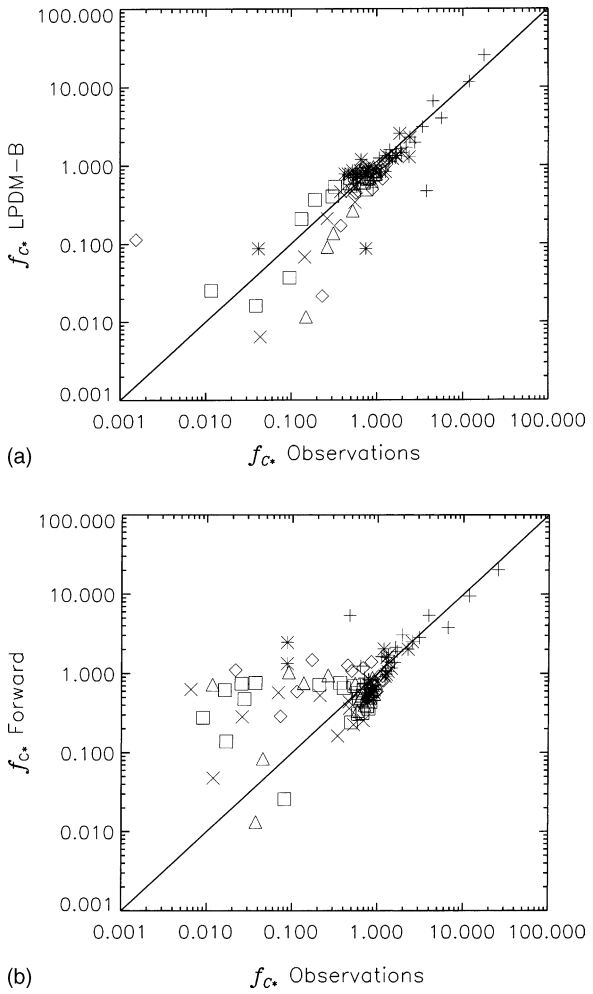

Fig. 5. Comparison of concentration footprints derived from the wind-tunnel with footprints predicted by (a) LPDM-B's 'backward-in-time' approach and (b) the 'forward-in-time' approach derived from DMOD's results. Measurement heights at $z_m/z_i = 0.09$ and 0.17 (+), 0.26 and 0.34 (*), 0.43 and 0.51 (◇), 0.60 and 0.69 (△), 0.77 and 0.89 (□), and 0.96 (×).

estimates at any height within the planetary boundary layer including the measurements above the surface layer.

For any of the measurement heights considered, the peak location of the footprint predicted by LPDM-B with the wind-tunnel fitted turbulence parameterisations was shifted slightly closer to the source than the estimate of LPDM-B with its original parameterisations. This behaviour is in accordance with the findings of Section 5.1, where the concentrations predicted by DMOD in original mode decreased more slowly than predicted by DMOD using fitted turbulence parameterisations. Even though the footprint estimates of LPDM-B agree better with the observations when implementing fitted turbulence parameterisations (Table 3), the footprint predictions of the two model versions did not differ significantly and exhibit very similar footprint shapes. Therefore it can be concluded, that at least for the present case, the footprint estimates were not as sensitive to the implemented turbulence parameterisations as the modelled dispersion. Since the turbulence characteristics of the wind tunnel compared well with atmospheric turbulence in a sheared convective boundary layer (Fedorovich et al., 1996), it can be further concluded that the turbulence parameterisations originally implemented in LPDM-B are well suited for footprint predictions in convective boundary layers.

The footprint estimates of the 'forward' approach and of LPDM-B ('backward' approach) correspond fairly well for the lowest measurement height ($z_m/z_i \approx 0.1$) (Fig. 4, solid and dotted lines). The 'forward' approach reproduced the observed peak value somewhat better than LPDM-B. For measurements higher above the surface, however, the footprints from the two approaches significantly differ (Fig. 4). When compared with the observations, the footprint peaks from the 'forward' approach were located too close to the measurement position. The discrepancy increased with the measurement height and was rather large for $z_m/z_i \geq 0.4$. As shown in Fig. 3, the concentration values at heights far above the surface ($z/z_i \geq 0.4$) can be over- or underestimated by the model by a factor of 20 or more, even if the general shape of the concentrations may be well represented. Hence, the 'forward' concentration footprint for large measurement heights was affected correspondingly. Fig. 5b and the summary statistics (Table 4) confirm these findings.

The differences revealed in footprint estimates from the 'forward' approach and the 'backward' approach of LPDM-B were rather surprising, since the flow patterns as applied in the two models were essentially the same. However, the 'forward' approach depends on the model's ability to simulate the concentration at the measurement height, z_m, from a

Table 4
Same as Table 3 but for the 'forward-in-time' approach

	$z_m/z_i \approx 0.1$		$z_m/z_i \approx 0.2$		$z_m/z_i \approx 0.5$		$z_m/z_i \approx 0.8$		Total	
	Fit	Orig	Fit	Orig	Fit	Orig	Fit	Orig	Fit	Orig
R	0.99	0.99	0.44	0.42	−0.16	0.08	0.07	0.77	0.95	0.95
F_2	100	100	91	82	64	73	55	64	67	74
F_B	0.04	0.07	−0.02	−0.02	−0.06	−0.05	−0.08	−0.06	−0.02	0.00
ε_{NMS}	0.05	0.08	0.72	0.81	0.49	0.41	0.67	0.17	0.12	0.14

ground-level source, while the 'backward' approach was dependent on how well the particle touchdown positions and the associated vertical velocities were modelled from a source at z_m.

For a Lagrangian particle model, the most delicate issues were the source conditions and the reflection scheme. As for the former, the 'forward' approach required a source height of $z = 0$ m, which was outside the physical range of a Lagrangian particle model and hence introduced some degree of arbitrariness. In the 'backward' approach, on the other hand, the footprint estimates were derived from a particle release farther above the ground, thus a release in a better-defined region. LPDM-B furthermore ran a spin-up procedure during initialisation resulting in realistic initial particle velocity distributions (Kljun et al., 2002). The reflection scheme influenced the results from both the 'forward' approach (critical since near the source) and the 'backward' approach (touchdown locations).

Clearly, the results as reported here were by no means general. If indeed the dispersion core of the model were perfect in the sense that it would yield the correct concentration distribution, associated with the correct velocity statistics, at any location in the domain and for any source height, then the 'forward' and the 'backward' approach should result in identical footprint estimates. It is also possible that using another dispersion core may reverse the observed relative performance of 'forward' and 'backward' approach. However, given the difficulty of Lagrangian particle models to realistically simulate a surface source and given the fact that dispersion models are usually validated using surface concentrations alone, a possible discrepancy between 'forward' and 'backward' approach is likely to increase with measurement height and may thus be important for concentration footprints of airborne measurements.

6. Summary and conclusions

The Lagrangian footprint model LPDM-B of Kljun et al. (2002) was evaluated using data from wind-tunnel experiments on dispersion in a sheared convective boundary layer. The wind-tunnel experiment was carried out at the University of Karlsruhe, Germany, releasing SF_6 as a tracer (Fedorovich and Thäter, 2002). The model evaluation was performed in three steps: a validation of the dispersion module of LPDM-B, an evaluation of footprint predictions of LPDM-B, and a comparison of two different footprint model approaches ('forward-in-time' and 'backward-in-time' trajectories).

The performed simulations showed that the dispersion module of LPDM-B successfully reproduced the basic features of the dispersion process. It was capable of not only reproducing surface concentration distributions, but also provided reliable concentration profiles throughout the boundary layer, at different downwind locations. The largest discrepancies between model predictions and observations were found close to the source location. It was suggested that differences in the source design of the model and of the wind-tunnel experiments may be responsible for these discrepancies.

Concentration footprints of LPDM-B compared well with the observations, both in peak location and shape. Summary statistics confirm the good performance of the model for measurement heights throughout the entire boundary layer. Given the fact that the dispersion module of LPDM-B has been successfully validated for convective, neutral and stable stratifications (Rotach et al., 1996; Rotach, 2001), it can be expected that footprint predictions for other stability conditions, beyond those for the present convective situation, would be of equal quality. It was also shown that the sensitivity of the footprint

predictions on the implemented turbulence statistics was not large. Using the original turbulence parameterisations rather than the observed characteristics did not significantly change the findings.

The comparison of LPDM-B's concentration footprints ('backward-in-time' trajectories) with respective estimates using the 'forward'-trajectories approach showed good correspondence for small measurement heights. However, farther above the surface, the agreement of footprint estimates from the 'forward' and the 'backward' approach was rather poor. The observed discrepancies increased with the measurement height. Thus using the same core model (dispersion module) did not necessarily result in identical concentration footprints. In the present case, the reason for the differences could be found in the height-dependence of the model performance. Only a perfect model with completely adequate dispersion for a ground-level source as well as for a source farther above the ground, and with perfect source and reflection simulation would yield identical footprint estimates. Therefore, it is important to carefully select and test the footprint model used for concentration footprints of airborne measurements.

The footprint predictions of LPDM-B with its implemented 'backward-in-time' trajectories approach compared very well with observations in the ideal, controlled conditions of the present wind-tunnel experiment. Further investigations should be carried out using wind-tunnel data for other boundary layer stabilities (neutral, stable), and finally with full-scale datasets for more complex conditions such as, for example, forest canopies or heterogeneous surfaces.

Acknowledgements

The authors would like to thank Johannes Thäter for his help with the wind-tunnel experiment, Pierluigi Calanca and three anonymous reviewers for their valuable comments on this manuscript, and the Biometeorology Group, University of British Columbia, Vancouver, Canada. This research was supported by the Swiss National Science Foundation (grant 8220-067600), by the European Commission and the Swiss Ministry of Education and Science (grant 97.0136) within the TMR-project TRAPOS, and by the Swiss Commission for Technology and Innovation (KTI) in the framework of EUROTRAC II (grants 3532.1 and 4092.1).

References

Baldocchi, D., 1997. Flux footprints within and over forest canopies. Boundary-Layer Meteorol. 85, 273–292.

Deardorff, J.W., 1985. Laboratory experiments on diffusion: the use of convective mixed-layer scaling. J. Appl. Meteorol. 24, 1143–1151.

de Haan, P., Rotach, M.W., 1998. A novel approach to atmospheric dispersion modelling: the Puff-particle model (PPM). Quart. J. Roy. Meteorol. Soc. 124, 2771–2792.

Fedorovich, E., Kaiser, R., Rau, M., Plate, E., 1996. Wind tunnel study of turbulent flow structure in the convective boundary layer capped by a temperature inversion. J. Atmos. Sci. 53, 1273–1289.

Fedorovich, E., Thäter, J., 2002. A wind tunnel study of gaseous tracer dispersion in the convective boundary layer capped by a temperature inversion. Atmos. Environ. 36, 2245–2255.

Finn, D., Lamb, B., Leclerc, M.Y., Horst, T.W., 1996. Experimental evaluation of analytical and Lagrangian surface-layer flux footprint models. Boundary-Layer Meteorol. 80, 283–308.

Flesch, T.K., 1996. The footprint for flux measurements, from backward Lagrangian stochastic models. Boundary-Layer Meteorol. 78, 399–404.

Flesch, T.K., Wilson, J.D., Yee, E., 1995. Backward-time Lagrangian stochastic dispersion models and their application to estimate gaseous emissions. J. Appl. Meteorol. 34, 1320–1332.

Hanna, S.R., Chang, J.C., Strimaitis, D.G., 1993. Hazardous gas model evaluation with field observations. Atmos. Environ. 27A, 2265–2281.

Horst, T.W., Weil, J.C., 1992. Footprint estimation for scalar flux measurements in the atmospheric surface layer. Boundary-Layer Meteorol. 59, 279–296.

Horst, T.W., Weil, J.C., 1994. How far is far enough? The fetch requirements for micrometeorological measurement of surface fluxes. J. Atmos. Ocean. Technol. 11, 1018–1025.

Kaharabata, S.K., Schuepp, P.H., Ogunjemiyo, S., Shen, S., Leclerc, M.Y., Desjardins, R.L., MacPherson, J.I., 1997. Footprint considerations in BOREAS. J. Geophys. Res. 102, 29113–29124.

Kaiser, R., Fedorovich, E., 1998. Turbulence spectra and dissipation rates in a wind tunnel model of the atmospheric convective boundary layer. J. Atmos. Sci. 55, 580–594.

Kljun, N., Kormann, R., Rotach, M.W., Meixner, F.X., 2003. Comparison of the Lagrangian footprint model LPDM-B with an analytical footprint model. Boundary-Layer Meteorol. 106, 349–355.

Kljun, N., Rotach, M.W., Schmid, H.P., 2002. A 3D backward Lagrangian footprint model for a wide range of boundary layer stratifications. Boundary-Layer Meteorol. 103, 205–226.

Kurbanmuradov, O., Sabelfeld, K., 2000. Lagrangian stochastic models for turbulent dispersion in the atmospheric boundary layer. Boundary-Layer Meteorol. 97, 191–218.

Leclerc, M.Y., Karipot, A., Prabha, T., Allwine, G., Lamb, B., Gholz, H.L., 2003a. Impact of non-local advection on flux footprints over a tall forest canopy: a tracer flux experiment. Agric. For. Meteorol. 115, 19–30.

Leclerc, M.Y., Meskhidze, N., Finn, D., 2003b. Comparison between measured tracer fluxes and footprint model predictions over a homogeneous canopy of intermediate roughness. Agric. For. Meteorol. 117, 145–158.

Leclerc, M.Y., Shen, S., Lamb, B., 1997. Observations and large-eddy simulation modeling of footprints in the lower convective boundary layer. J. Geophys. Res. 102, 9323–9334.

Leclerc, M.Y., Thurtell, G.W., 1990. Footprint prediction of scalar fluxes using a Markovian analysis. Boundary-Layer Meteorol. 52, 247–258.

Mason, P.J., 1992. Large-eddy simulation of dispersion in convective boundary layers with wind shear. Atmos. Environ. 26A, 1561–1571.

Rannik, U., Aubinet, M., Kurbanmuradov, O., Sabelfeld, K.K., Markkanen, T., Vesala, T., 2000. Footprint analysis for measurements over a heterogeneous forest. Boundary-Layer Meteorol. 97, 137–166.

Rotach, M.W., 2001. Urban-scale dispersion modeling taking into account the turbulence and flow characteristics of the roughness sublayer. In: Proceedings of the 3rd International Symposium on Environmental Hydraulics, Tempe, Arizona.

Rotach, M.W., Gryning, S.-E., Tassone, C., 1996. A two-dimensional Lagrangian stochastic dispersion model for daytime conditions. Quart. J. Roy. Meteorol. Soc. 122, 367–389.

Schmid, H.P., 2002. Footprint modeling for vegetation atmosphere exchange studies: a review and perspective. Agric. For. Meteorol. 113, 159–184.

Schuepp, P.H., Leclerc, M.Y., Macpherson, J.I., Desjardins, R.L., 1990. Footprint prediction of scalar fluxes from analytical solutions of the diffusion equation. Boundary-Layer Meteorol. 50, 355–373.

Thomson, D.J., 1987. Criteria for the selection of stochastic models of particle trajectories in turbulent flows. J. Fluid Mech. 180, 529–556.

Van Ulden, A.P., 1978. Simple estimates for vertical diffusion from sources near the ground. Atmos. Environ. 12, 2125–2129.

Willis, G.E., Deardorff, J.W., 1976. A laboratory model of diffusion into the convective planetary boundary layer. Quart. J. Roy. Meteorol. Soc. 102, 427–445.

Willis, G.E., Deardorff, J.W., 1978. A laboratory study of dispersion from an elevated source within a modelled convective planetary boundary layer. Atmos. Environ. 12, 1305–1311.

Willis, G.E., Deardorff, J.W., 1981. A laboratory study of dispersion from a source in the middle of the convective layer. Atmos. Environ. 15, 109–117.

Wilson, J.D., Swaters, G.E., 1991. The source area influencing a measurement in the planetary boundary layer: The ‘‘footprint’’ and the ‘‘distribution of contact distance’’. Boundary-Layer Meteorol. 55, 25–46.